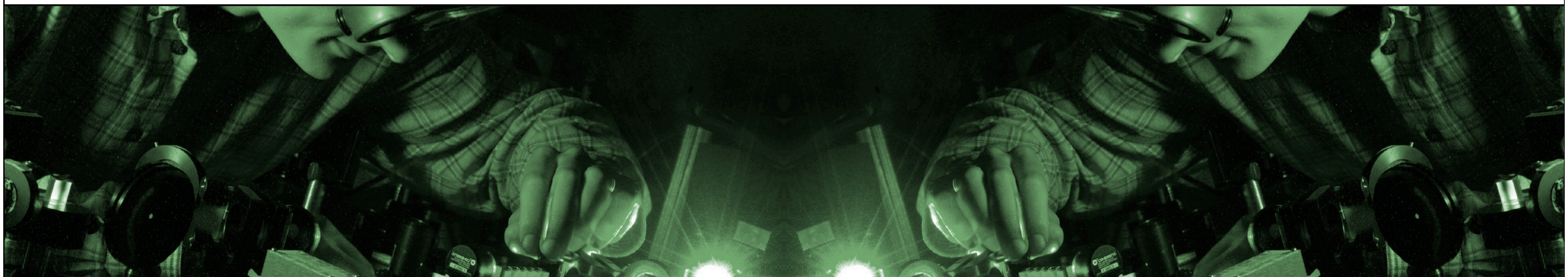

November 17, 2008

Ghost Imaging: From Quantum to Classical to Computational

Jeffrey H. Shapiro

Research sponsored by the U.S. Army Research Office,
the Defense Advanced Research Projects Agency, and
the W. M. Keck Foundation Center for Extreme Quantum Information theory

Optical and Quantum Communications Group

The Truth about Ghost Imaging

- Biphoton ghost imaging
- Pseudothermal ghost imaging
- Unified Gaussian-state resolution and field-of-view analysis
- Signal-to-noise ratio behavior
- Spatial light modulator (SLM) ghost imaging
- Computational ghost imaging
- Potential for aberration immunity
- Discussion

SPDC and the Biphoton State

- Spontaneous parametric downconversion (SPDC)

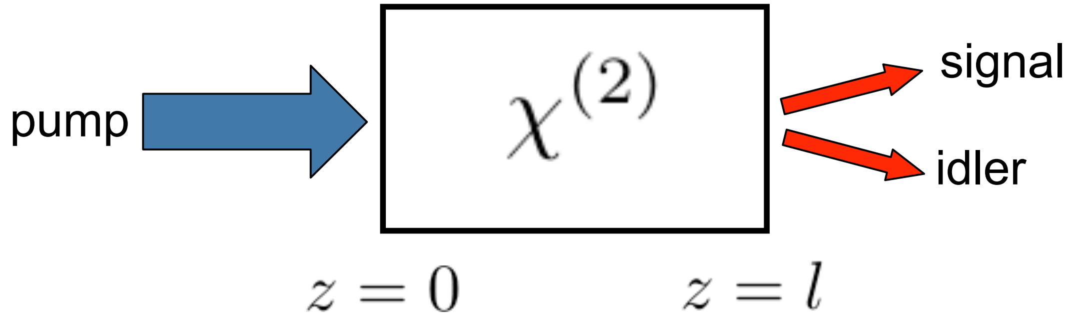

  - strong pump at frequency ω_P
  - no input at signal frequency ω_S or at idler frequency ω_I
  - nonlinear mixing produces signal and idler outputs that are *entangled* in frequency and momentum

$$\omega_P = \omega_S + \omega_I \text{ and } \boldsymbol{k}_P = \boldsymbol{k}_S + \boldsymbol{k}_I$$

  - with type-II phase matching signal and idler are orthogonally polarized
  - at low flux these entangled outputs form a stream of biphotons

Ghost Imaging in the Biphoton Limit

- Pittman *et al*. ghost imaged a transmission mask
  - used biphoton-state source and coincidence counting
  - it's a ghost image because the bucket detector has no spatial resolution and the object is not in the path of the pinhole detector
  - attributed this behavior to entanglement of signal and idler photons

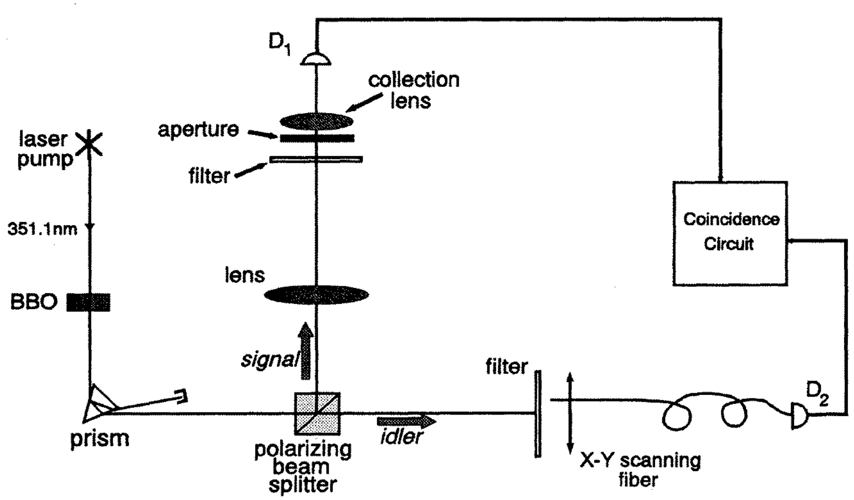

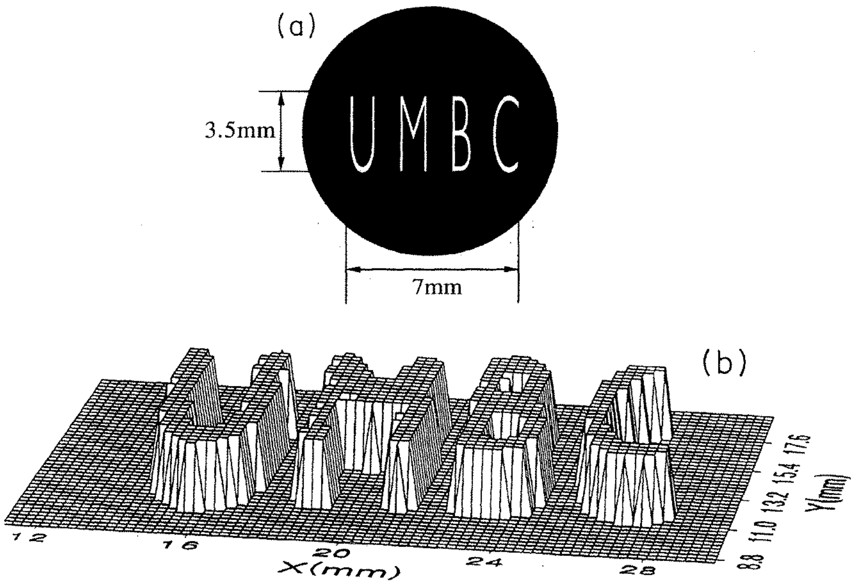

Pittman *et al.*
Phys Rev A 1995

Pseudothermal Ghost Imaging

- Scarcelli *et al*. ghost imaged a transmission mask
  - used pseudothermal light and photocurrent correlation
  - it's a ghost image because the bucket detector has no spatial resolution and the object is not in the path of the pinhole detector
  - attributed this behavior to nonlocal two-photon interference

Ghost Image - Near Field

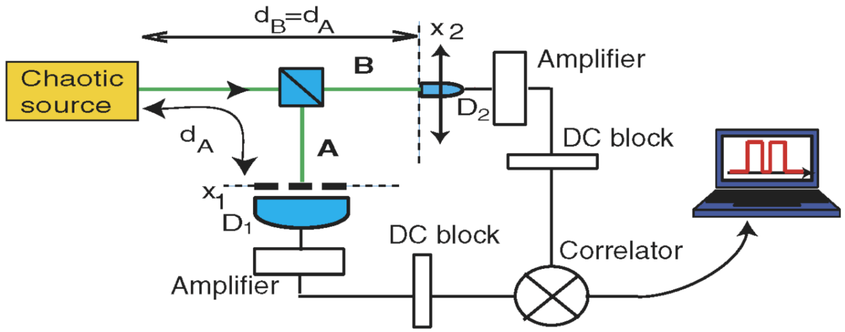

Object

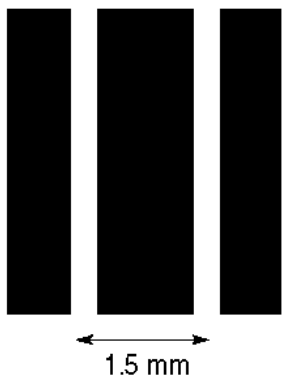

Image

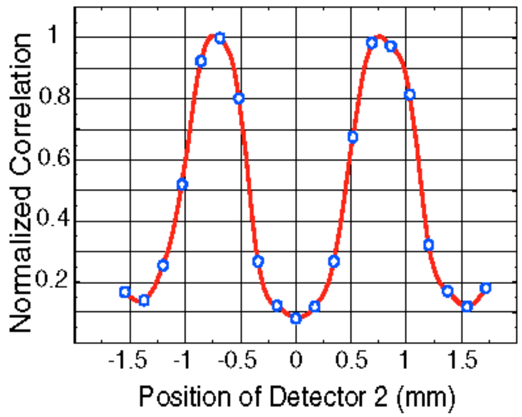

Scarcelli *et al*.
***Phys Rev Lett* 2006**

The Toy Soldier

- Meyers *et al*. ghost imaged a toy soldier
  - used pseudothermal light and coincidence counting
  - it's a ghost image because the bucket detector has no spatial resolution and the object is not in the path of the CCD array
  - attributed this behavior to nonlocal two-photon interference

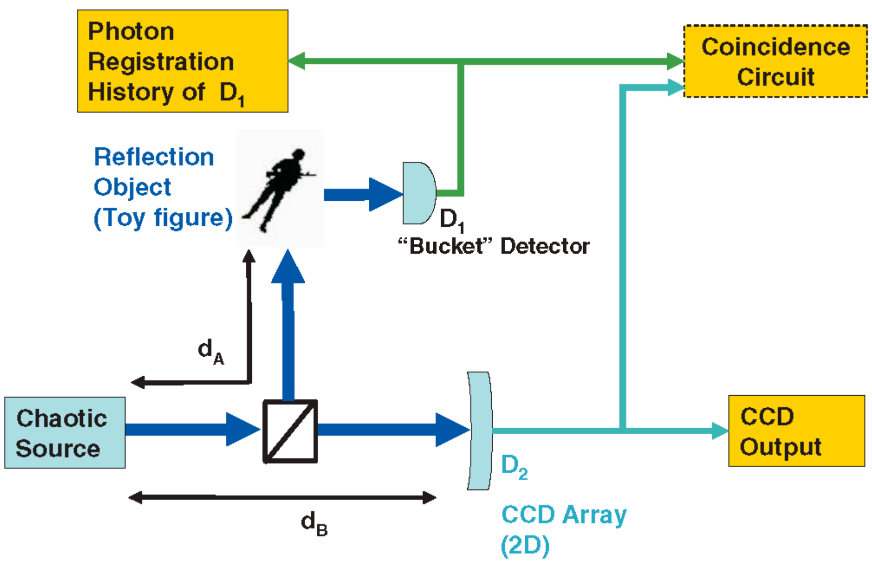

Meyers *et al*.
***Phys Rev A* 2008**

Classical versus Quantum Imaging

- High-sensitivity photodetection is…
  - *always* quantum, because light is quantum mechanical and photodetection is a quantum measurement
- High-sensitivity photodetection performance may often be…
  - *calculated* semiclassically, by assuming light is classical and the electron charge is discrete, so that the noise behavior is Poisson shot noise plus classical-light excess noise
- Semiclassical theory is quantitatively correct…
  - when light is in a coherent state or a mixture thereof and standard photodetection (direct, homodyne, or heterodyne) is employed
- Imaging performance is truly quantum *if*…
  - it cannot be explained by semiclassical theory

Unified Gaussian-State Framework

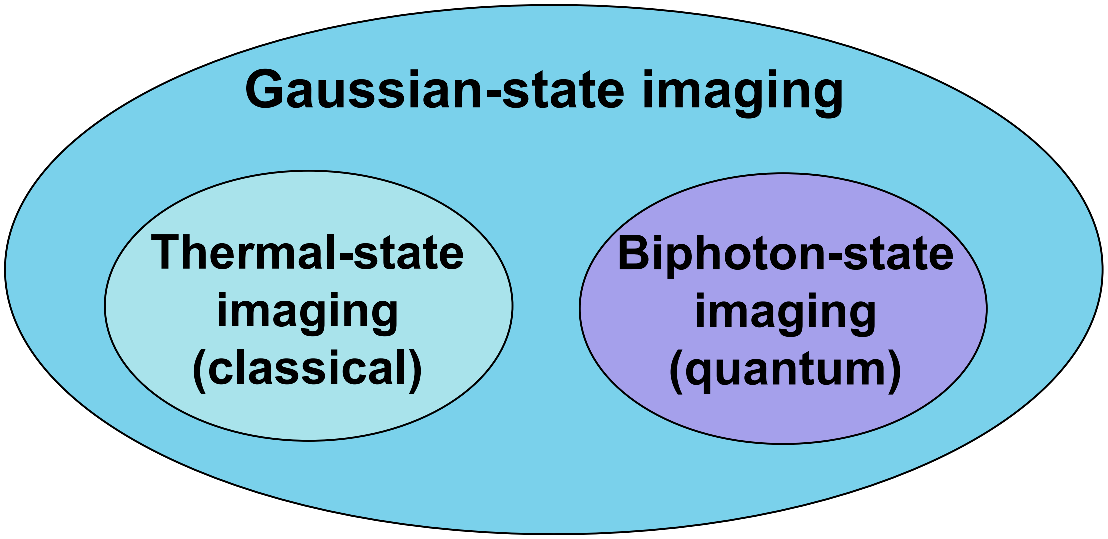

- Gaussian states include…
  - laser light, LED light, sunlight, i.e., "classical states"
  - low-flux biphoton output from SPDC, viz., a "quantum" state
- Gaussian states are…
  - characterized by their mean values and coherence functions
  - closed under linear transformations like free-space diffraction

Zero-Mean Gaussian States

- Positive-frequency, photon-units field operator: $\hat{E}_z(\boldsymbol{\rho}, t)e^{ik_0 z - i\omega_0 t}$
  - paraxial, z-propagating
  - $[\hat{E}_z(\boldsymbol{\rho}_1, t_1), \hat{E}_z^\dagger(\boldsymbol{\rho}_2, t_2)] = \delta(\boldsymbol{\rho}_2 - \boldsymbol{\rho}_1)\delta(t_2 - t_1)$
- Zero-mean Gaussian state completely characterized by
  - phase-insensitive correlation function: $\langle \hat{E}_z^\dagger(\boldsymbol{\rho}_1, t_1)\hat{E}_z(\boldsymbol{\rho}_2, t_2)\rangle$
  - phase-sensitive correlation function: $\langle \hat{E}_z(\boldsymbol{\rho}_1, t_1)\hat{E}_z(\boldsymbol{\rho}_2, t_2)\rangle$
- *If* $\langle \hat{E}_z(\boldsymbol{\rho}_1, t_1)\hat{E}_z(\boldsymbol{\rho}_2, t_2)\rangle = 0$
  - state is always classical (has proper *P*-representation)
  - laser light, LED light, thermal light
- *If* $\langle \hat{E}_z(\boldsymbol{\rho}_1, t_1)\hat{E}_z(\boldsymbol{\rho}_2, t_2)\rangle \neq 0$
  - state may be classical or nonclassical
  - squeezed light, classical phase-sensitive light

Quantum Huygens-Fresnel Principle Propagation

- Correlation propagation from $z = 0$ to $z = L$

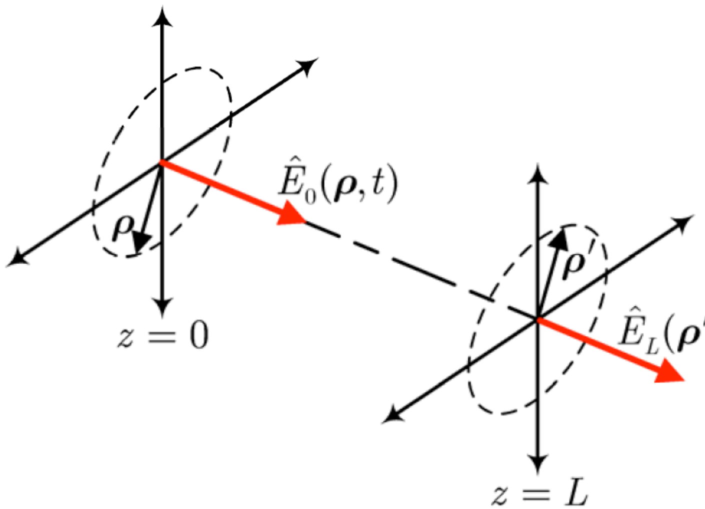

Huygens-Fresnel principle

$$\hat{E}_L(\boldsymbol{\rho}', t) = \int \mathrm{d}\boldsymbol{\rho}\, \hat{E}_0(\boldsymbol{\rho}, t - L/c) \underbrace{\frac{\exp(ik_0|\boldsymbol{\rho}' - \boldsymbol{\rho}|^2/2L)}{i\lambda_0 L}}_{h_L(\boldsymbol{\rho}' - \boldsymbol{\rho})}$$

$$K_L^{(p)}(\boldsymbol{\rho}_1', \boldsymbol{\rho}_2', \tau) \equiv \langle \hat{E}_L(\boldsymbol{\rho}_1', t + \tau)\hat{E}_L(\boldsymbol{\rho}_2', t)\rangle$$

$$K_L^{(p)}(\boldsymbol{\rho}_1', \boldsymbol{\rho}_2', \tau) = \int\!\!\int \mathrm{d}\boldsymbol{\rho}_1\, \mathrm{d}\boldsymbol{\rho}_2\, K_0^{(p)}(\boldsymbol{\rho}_1, \boldsymbol{\rho}_2, \tau) h_L(\boldsymbol{\rho}_1' - \boldsymbol{\rho}_1) h_L(\boldsymbol{\rho}_2' - \boldsymbol{\rho}_2)$$

$$K_L^{(n)}(\boldsymbol{\rho}_1', \boldsymbol{\rho}_2', \tau) \equiv \langle \hat{E}_L^{\dagger}(\boldsymbol{\rho}_1', t + \tau)\hat{E}_L(\boldsymbol{\rho}_2', t)\rangle$$

$$K_L^{(n)}(\boldsymbol{\rho}_1', \boldsymbol{\rho}_2', \tau) = \int\!\!\int \mathrm{d}\boldsymbol{\rho}_1\, \mathrm{d}\boldsymbol{\rho}_2\, K_0^{(n)}(\boldsymbol{\rho}_1, \boldsymbol{\rho}_2, \tau) h_L^{*}(\boldsymbol{\rho}_1' - \boldsymbol{\rho}_1) h_L(\boldsymbol{\rho}_2' - \boldsymbol{\rho}_2)$$

Gaussian-State Correlation Functions

- Gaussian Schell-model phase-insensitive auto-correlation

$$\langle \hat{E}_\ell^\dagger(\boldsymbol{\rho}_1, t_1)\hat{E}_\ell(\boldsymbol{\rho}_2, t_2)\rangle = \frac{2P}{\pi a_0^2} e^{-(|\boldsymbol{\rho}_1|^2+|\boldsymbol{\rho}_2|^2)/a_0^2 - |\boldsymbol{\rho}_2-\boldsymbol{\rho}_1|^2/2\rho_0^2} e^{-(t_2-t_1)^2/2T_0^2}$$

$\ell = S, R$

P: photon flux; a_0: beam radius >> ρ_0: coherence length; T_0: coherence time

- Thermal (and pseudothermal) light
  - phase-insensitive cross-correlation = phase-insensitive auto-correlation
  - no phase-sensitive auto-correlation or cross-correlation

- Phase-sensitive light
  - no phase-insensitive cross-correlation
  - no phase-sensitive auto-correlation
  - maximum quantum phase-sensitive cross-correlation

Biphoton Ghost Imaging

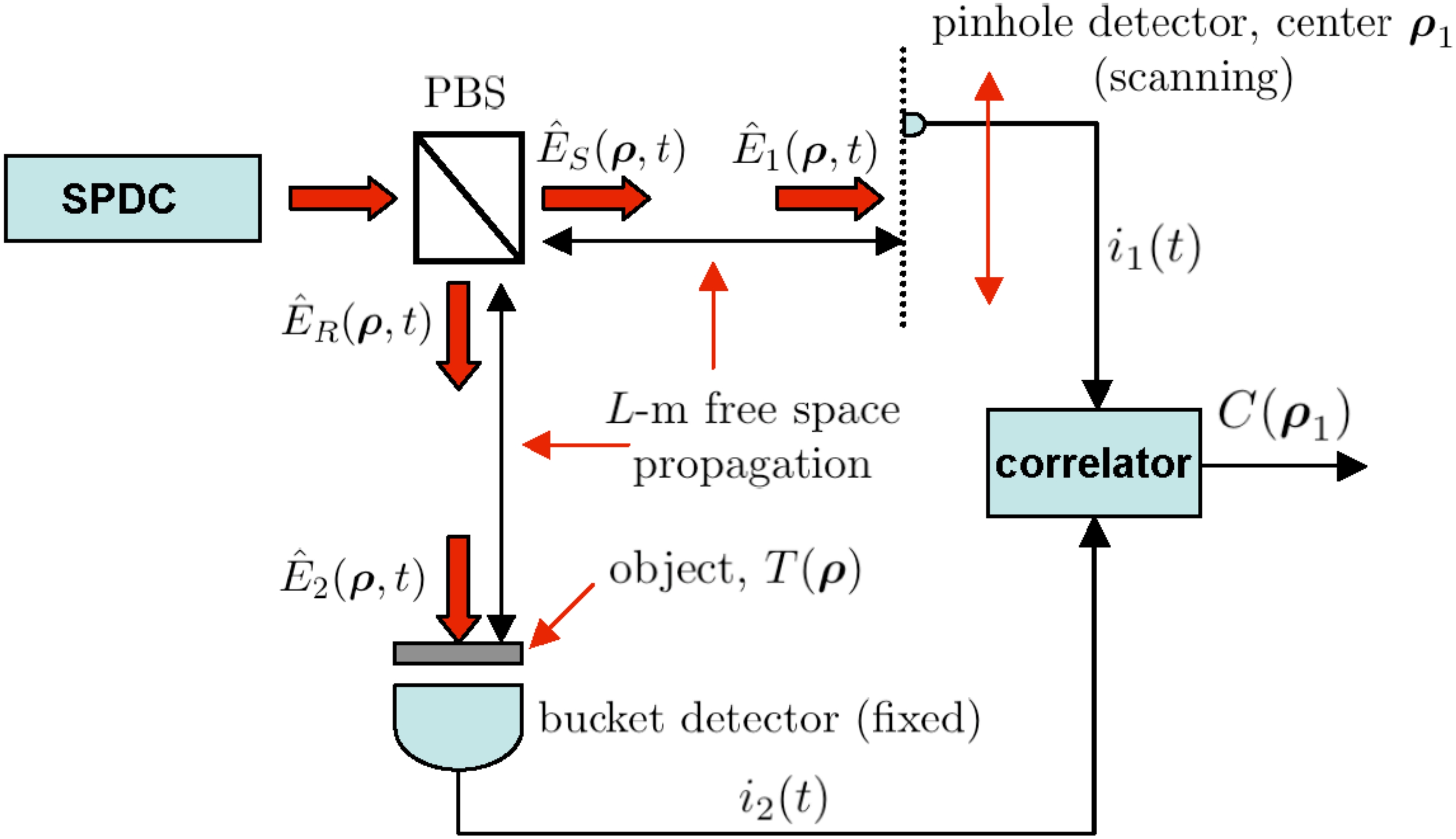

Biophoton Ghost Imaging

- Assume Gaussian-Schell model source:

  photon flux P, intensity radius a_0, coherence radius $\rho_0 \ll a_0$

- Assume far-field operation: $k_0 a_0^2/2L \ll 1$
- Assume object lies within $\sqrt{2}\lambda_0 L/\pi\rho_0$ field of view
- Photocurrent cross-correlation function

$$
\begin{aligned}
C(\boldsymbol{\rho}_1) \;=\;& q^2 \eta_1 \eta_2 A_1 \left(\frac{2P}{\pi a_L^2}\right)^2 \left[\int_{\mathcal{A}_2} d\boldsymbol{\rho}\, |T(\boldsymbol{\rho})|^2 \right. \\
&+ \left. \sqrt{\frac{1}{8\pi}} \frac{a_0^2}{P T_0 \rho_0^2} \int_{\mathcal{A}_2} d\boldsymbol{\rho}\, e^{-|\boldsymbol{\rho}_1 + \boldsymbol{\rho}|^2/\rho_L^2} |T(\boldsymbol{\rho})|^2 \right]
\end{aligned}
$$

intensity radius $a_L = \lambda_0 L/\pi\rho_0$, coherence radius $\rho_L = \lambda_0 L/\pi a_0$

Erkmen & Shapiro, *PRA* (2008)

Pseudothermal Ghost Imaging

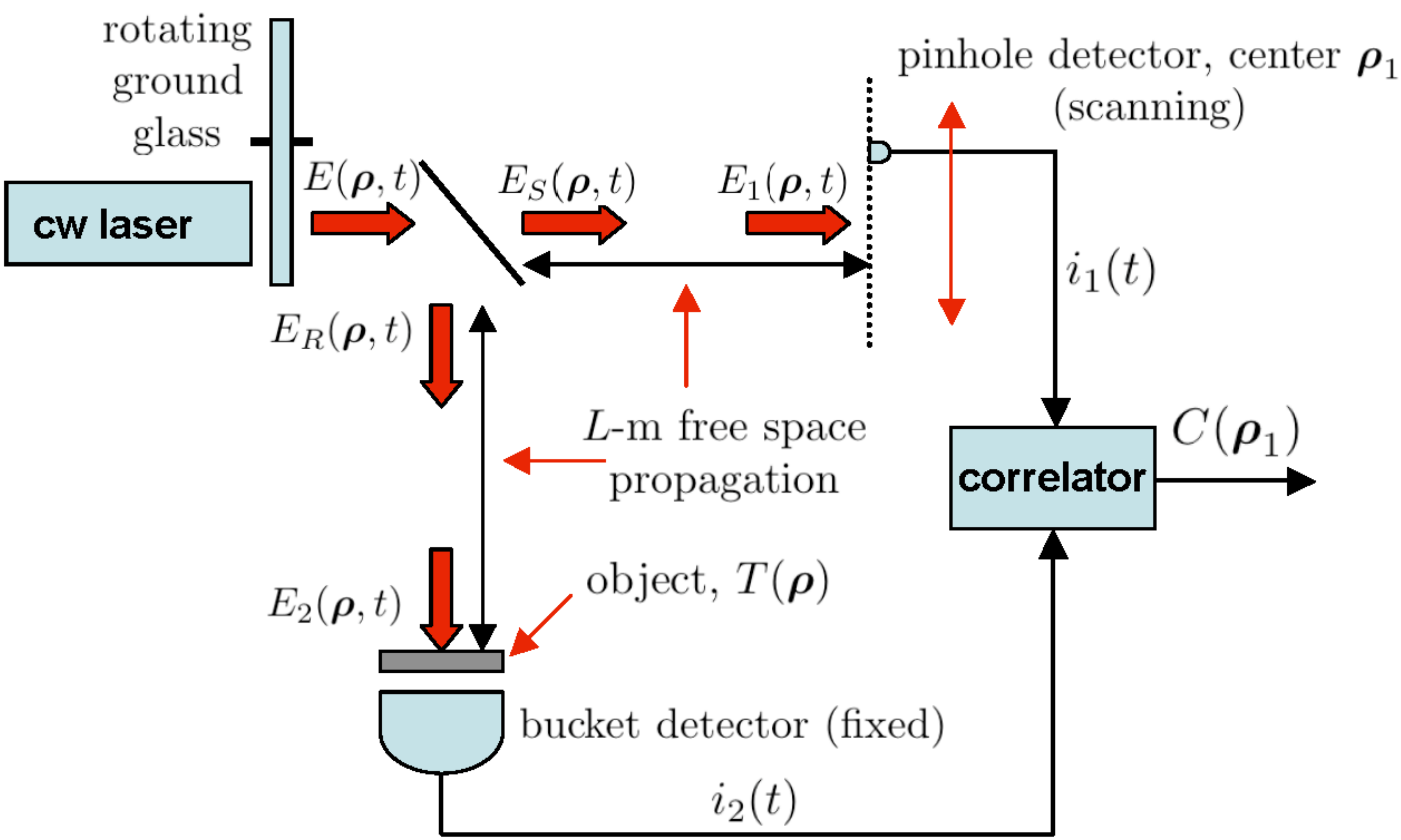

Pseudothermal Ghost Imaging

- Assume Gaussian-Schell model source:

  photon flux P, intensity radius a_0, coherence radius $\rho_0 \ll a_0$

- Assume far-field operation: $k_0 a_0 \rho_0 / 2L \ll 1$
- Assume object lies within $\lambda_0 L/\pi\rho_0$ field of view
- Photocurrent cross-correlation function

$$\begin{aligned} C(\boldsymbol{\rho}_1) &= q^2 \eta_1 \eta_2 A_1 \left(\frac{2P}{\pi a_L^2}\right)^2 \left[\int_{\mathcal{A}_2} d\boldsymbol{\rho}\, |T(\boldsymbol{\rho})|^2 \right. \\ &+ \left. \int_{\mathcal{A}_2} d\boldsymbol{\rho}\, e^{-|\boldsymbol{\rho}_1 - \boldsymbol{\rho}|^2/\rho_L^2} |T(\boldsymbol{\rho})|^2 \right] \end{aligned}$$

intensity radius $a_L = \lambda_0 L/\pi\rho_0$, coherence radius $\rho_L = \lambda_0 L/\pi a_0$

Erkmen & Shapiro, *PRA* (2008)

Dual-Wavelength Operation

- Assume Gaussian-Schell model source

  photon flux P, intensity radius a_0, coherence radius $\rho_0 \ll a_0$

- Use nondegenerate type-II SPDC

  signal frequency ω_S, idler frequency ω_I

- Use unequal path lengths

  signal path length L_S, idler path length L_I

- Assume far-field operation: $k_S a_0^2/2L_S, k_I a_0^2/2L_I \ll 1$
- Image is focus when $k_S/L_S = k_I/L_I$
- Spatial resolution set by $\lambda_S L_S/\pi\rho_0 = \lambda_I L_I/\pi\rho_0$

What about Signal-to-Noise Ratio?

- Source coherence time: T_0
- Photodetector response time: T_d
- Cross-correlation integration time: T_I
- Broadband biphoton imaging: $T_0 \ll T_d \ll T_I$

$$\text{SNR} \longrightarrow \frac{2\eta_1\eta_2 P T_I A_1}{\pi a_L^2} |T(\boldsymbol{\rho}_1)|^2 \text{ with increasing } P$$

but *only* in the biphoton limit

- Narrowband pseudothermal imaging: $T_d \ll T_0 \ll T_I$

$$\text{SNR} \longrightarrow \sqrt{2\pi} \frac{T_I}{T_0} \frac{\rho_L^2}{A'_T} |T(\boldsymbol{\rho}_1)|^4 \text{ with increasing } P$$

$$A'_T = \text{effective area of object}$$

Erkmen & Shapiro
arXiv:0809.4167 [quant-ph]

What about Image Acquisition Time?

- Image acquisition time (T_I) is the averaging time needed to achieve a target value for SNR

- Comparison between broadband biphoton source ($T_I^{(q)}$) and narrowband pseudothermal source ($T_I^{(c)}$)

$$\frac{T_I^{(q)}}{T_I^{(c)}} = \frac{\sqrt{\pi^3/2}}{\eta_1\eta_2 P^{(q)} T_0^{(c)}} \frac{a_L^2}{A'_T} \frac{\rho_L^2}{A_1} |T(\boldsymbol{\rho}_1)|^2$$

- Depending on parameter values, comparison may favor either source

- *BUT*, broadband biphoton source is extremely vulnerable to background light, whereas narrowband pseudothermal source is not

Erkmen & Shapiro
arXiv:0809.4167 [quant-ph]

Spatial Light Modulator Ghost Imaging

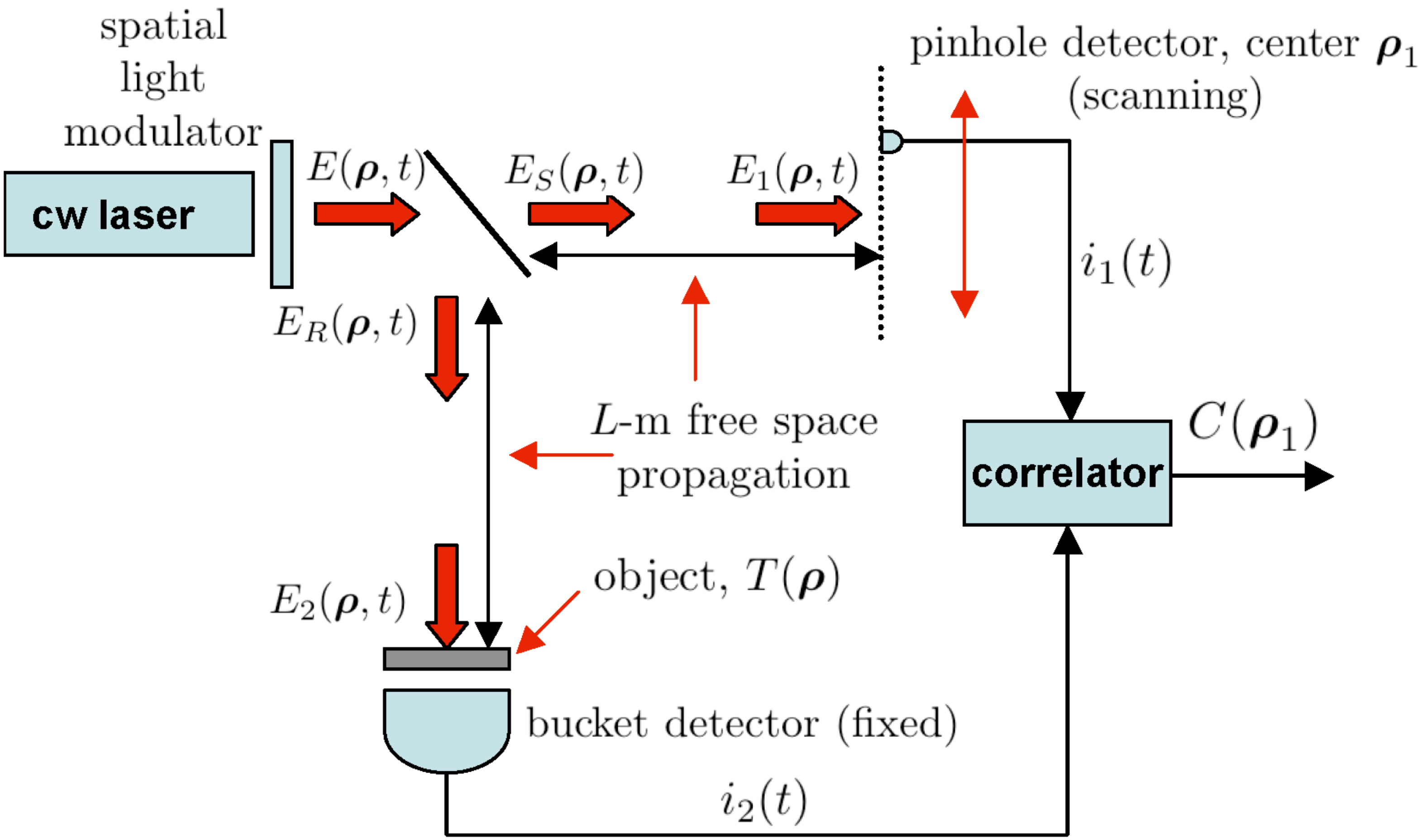

Shapiro, arXiv:0807.2614 [quant-ph]

Spatial Light Modulator Ghost Imaging

- Assume SLM is $(2M+1)\text{x}(2M+1)$ array
  - dxd pixels, 100% fill factor, $D = (2M+1)d$, $M >> 1$
- Apply random phase modulation to each pixel
- Measurement plane spatial correlation function

$$K'(\boldsymbol{\rho}_1, \boldsymbol{\rho}_2) = \frac{P}{2}\left(\frac{d^2}{D\lambda_0 L}\right)^2 e^{ik_0(|\boldsymbol{\rho}_2|^2 - |\boldsymbol{\rho}_1|^2)/2L}$$

$$\times \left(\prod_{u=x,y} \frac{\sin(k_0 d u_1/2L)}{k_0 d u_1/2L}\frac{\sin(k_0 d u_2/2L)}{k_0 d u_2/2L}\right)$$

$$\times \left(\prod_{u=x,y} \frac{\sin[k_0 D(u_1 - u_2)/2L]}{\sin[k_0 d(u_1 - u_2)/2L]}\right)$$

Spatial Light Modulator Ghost Imaging

- Photocurrent cross-correlation function

$$
\begin{aligned}
C(\boldsymbol{\rho}_1) \;&=\; q^2\eta_1\eta_2 A_1 K'(\boldsymbol{\rho}_1,\boldsymbol{\rho}_1)\int_{\mathcal{A}_2} d\boldsymbol{\rho}\, K'(\boldsymbol{\rho},\boldsymbol{\rho})|T(\boldsymbol{\rho})|^2 \\
&+\; q^2\eta_1\eta_2 A_1 \int_{\mathcal{A}_2} d\boldsymbol{\rho}\, |K'(\boldsymbol{\rho}_1,\boldsymbol{\rho})|^2|T(\boldsymbol{\rho})|^2
\end{aligned}
$$

- Assume object lies within $\lambda_0 L/d$ field of view
- Ghost image has spatial resolution $\lambda_0 L/D$
- Featureless background can be eliminated
  - use DC block on either photodetector

Computational Ghost Imaging

- Spatial light modulator ghost imaging can use deterministic phase modulation:

- Evaluate diffraction integral off-line in advance

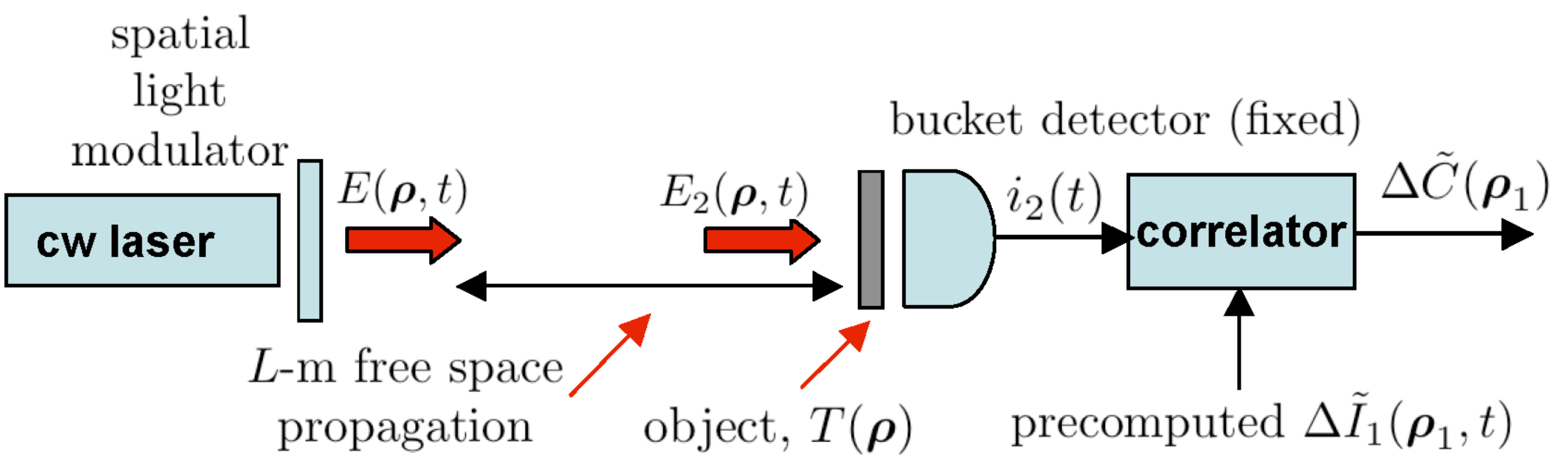

- Obtain single-beam ghost image

$$\text{field of view} = \lambda_0 L/d, \text{ spatial resolution} = \lambda_0 L/D$$

Shapiro, arXiv:0807.2614 [quant-ph]

Computational Ghost Imaging

- One light beam and one photodetector
  - *no* nonlocal two-photon interference can occur

- Depth of focus for range-spread reflectance
  - pseudothermal case

$$|\Delta L|/L = 4L/k_0 a_0^2 \ll 1 \text{ in near field of cw laser}$$

    - each focal region must be imaged separately

  - computational case

$$|\Delta L|/L \approx L/k_0 D^2 \ll 1 \text{ in near field of cw laser}$$

    - many focal regions may be imaged at once

What about Atmospheric Turbulence?

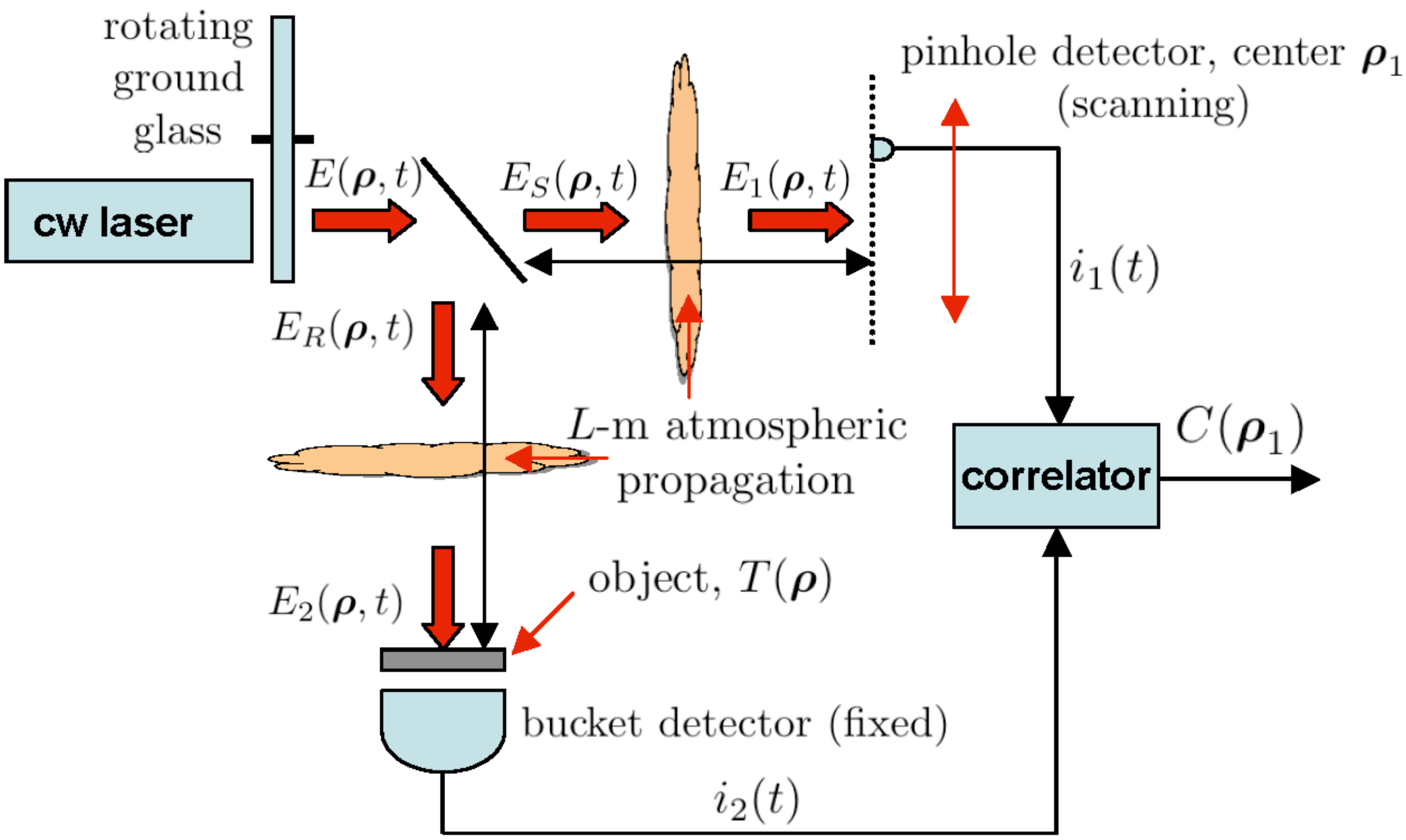

Potential for Aberration Immunity

- Turbulence only between object and bucket
  - no loss of resolution
- Identical turbulence on both paths
  - no loss of resolution
- Statistically identical turbulence on both paths
  - resolution becomes turbulence limited
- Turbulence only between source and bucket
  - resolution becomes turbulence limited
- Turbulence only between source and pinhole detector
  - resolution becomes turbulence limited

Discussion

- Partially coherent light creates speckle patterns
  - speckle size ~ wavelength x path length/source size

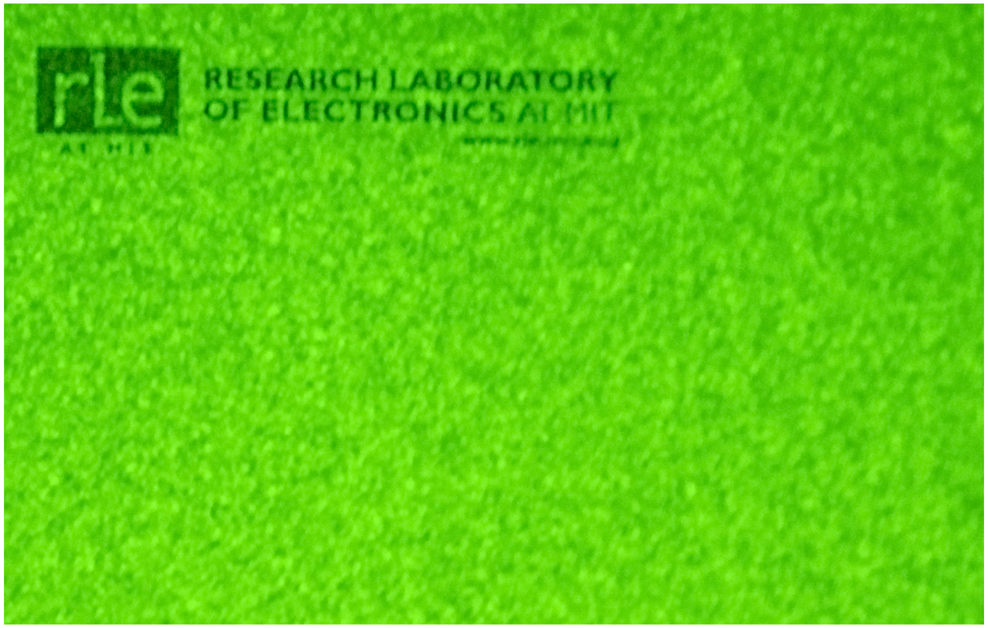

- Ghost imaging is speckle pattern cross correlation
  - high-resolution images require *very small* speckles

Discussion

- Active two-beam ghost imaging
  - uses active illuminator to cast correlated speckle patterns
  - biphoton source: low brightness, low flux
  - pseudothermal source: high brightness, high flux
  - SLM source: controllable spatial coherence
- Active single-beam ghost imaging
  - uses precomputed high-resolution speckle pattern
  - only needs a bucket detector
  - can ghost image at wavelengths for which cameras unavailable
- Passive ghost imaging
  - uses natural-illumination speckle patterns
  - broadband operation yields very low image contrast
  - passive imaging without beam splitter requires *very large* speckles
- Ghost imaging has limited potential for aberration immunity

Other Work...

- Far-field diffraction pattern imaging

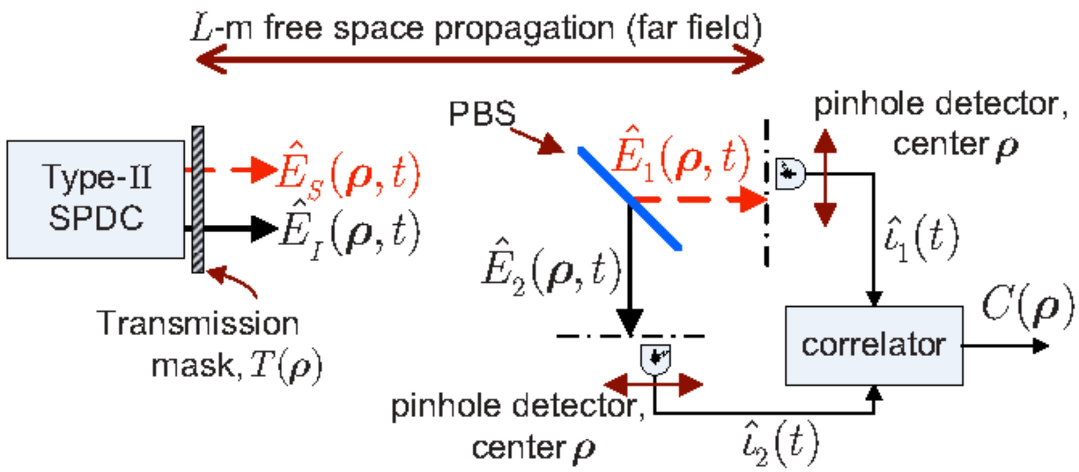

- Two-photon imaging

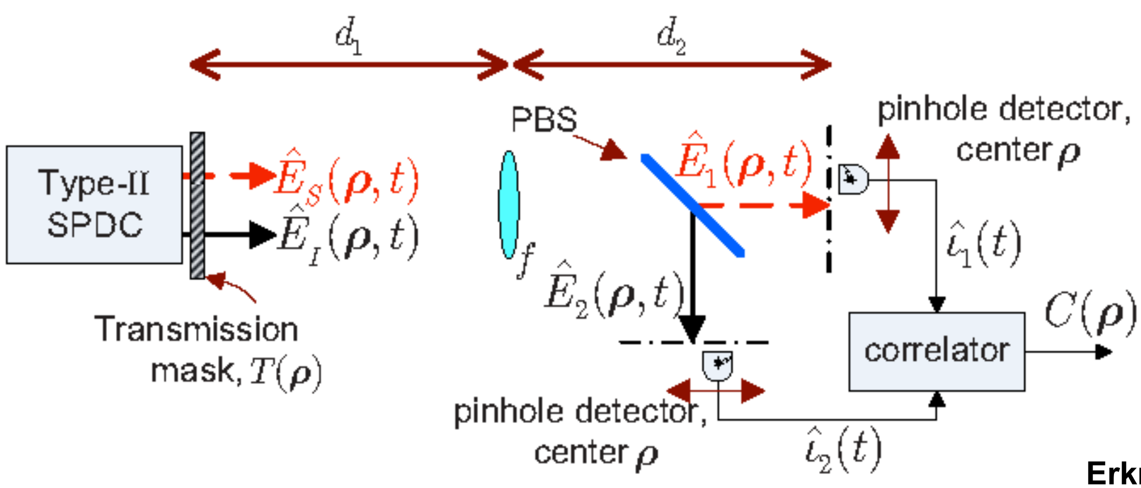

Erkmen & Shapiro, *PRA* (2008)

Future Work...

- Franco Wong will collaborate on experiments
- Two 512 x 512 SLMs have been purchased
- Quantitative ghost imaging experiments will be performed
- Will study field-of-view, resolution, and signal-to-noise ratio
- Will study classical phase-insensitive noise
- Will study classical phase-sensitive noise
- Will study nonclassical phase-sensitive noise